Improving Hosting Capacity of Unbalanced Distribution Networks via Robust Allocation of Battery Energy Storage Systems

Bo Wang, *Student Member, IEEE*, Cuo Zhang, *Member, IEEE*, Zhao Yang Dong, *Fellow, IEEE*, and Xuejun Li

***Abstract*—Distribution system operators aim to improve hosting capacity (HC) of distribution networks (DNs) to accommodate more distributed rooftop photovoltaics (PVs). Although PV power generation delivers numerous benefits, power unbalance and voltage rise are two major obstacles that limit the network HC. To mitigate these issues, battery energy storage systems (BESSs) can be applied. Thus, this paper proposes a robustly optimal allocation method for BESSs, which aims to reduce the power unbalance and alleviate the voltage rise, and thus improve the HC of the unbalanced three-phase DNs. Considering that locations and capacities of distributed rooftop PVs are determined by customers, future PV installations are regarded as uncertainties. In addition, to deal with the uncertainties, the proposed BESS allocation problem is formulated as an adaptive robust optimization (ARO) model with integer recourse variables. Accordingly, a solution algorithm which integrates an alternating optimization procedure into a column-and-constraint generation algorithm is developed to efficiently solve the ARO model. With the proposed BESS allocation method, a new perspective on HC improvement is provided, which not only considers the worst power unbalance situation but also satisfies the allowed maximum PV capacity. The simulation results verify high efficiency and solution robustness of the proposed allocation method.**

***Index Terms*-- Adaptive robust optimization, battery energy storage system, hosting capacity, mixed integer linear programming, unbalanced distribution network.**

NOMENCLATURE

A. Sets and Indices

N, n	Set/Index of buses in distribution network.
I, i	Set/Index of candidate buses where battery energy storage systems (BESSs) or distributed rooftop PVs will be installed, $I \in N$.
G, g	Set/Index of buses where PVs have been installed, $G \in N$.
P, p	Set/Index of phases a, b, c.
T, t	Set/Index of time intervals.

B. Parameters

$BSNo$	Maximum number of BESS modules for installation.
E_i^{cap}	BESS capacity (kWh).
K_i	Maximum number of BESS modules that can be installed at each candidate bus.
P_{max}^{TF}	Maximum transformer power limit at each phase.
$P_{rate,i}^{ch/dis}$	Rated charging/discharging power (kW) of BESS module at each phase.
$SoC_{min/max}$	Minimum/Maximum BESS state of charge (%).
UNB_{max}	Hourly maximum unbalance limit (p.u.).
$V_{min/max}$	Minimum/Maximum voltage limits (p.u.).
$\bar{z}_{n\to n+1}$	Equivalent branch impedance from bus n to n+1,
γ	BESS energy leakage factor (%).
δ_t	Average PV generation profiles at time t
$\underline{\mu}_p$ $\overline{\mu}_p$	Lower/Upper bounds of uncertainty budget at each phase.
$(\tilde{\cdot})$	Uncertainties including existing PV generation /load/future PV installations.
$(\underline{\cdot})$ $(\overline{\cdot})$	Lower/Upper bounds of uncertainty.
$(\hat{\cdot})$	Expected value of uncertainty

C. Variables

$E_{i,t}^{BS}$	Stored energy in the BESS (kWh).
$P/Q_{n,p,t}^{LD}$	Active/Reactive power of load (kW/kVar).
$P_{i,p,t}^{BS}$	BESS internal power (kW).
$P_{i,p,t}^{ch/dis}$	BESS charging/discharging power (kW).
$P_{i,p}^{FPV}$	Capacity of future PV installations.
$P_{g,p,t}^{PV}$	Existing PV power generation.
P_t^{unb}	Root branch active power unbalance
$P/Q_{n,p,t}^{br}$	Branch active/reactive power flow from bus n. $P/Q_{1,p,t}^{br}$ denotes active/reactive power flow from transformer.
$v_{n,p,t}$	Square of bus voltage magnitude (p.u.).
α_i	Integer variable of BESS allocation at bus i.
$\beta_{i,t}$	Binary variable of BESS operation state

I. INTRODUCTION

The rapid growth of renewable distributed generation (DG) brings numerous benefits in economic, technical and environmental aspects. In distribution networks (DNs), the penetration of distributed rooftop solar photovoltaics (PVs), as renewable DG, is significantly high. Although distribution

The work was supported in part by ARC Research Hub for Integrated Energy Storage Solutions (IH180100020), and in part by UNSW Digital Grid Futures Institute. The work of B. Wang was supported by UNSW-CSIRO Industry PhD program. *(Corresponding author: Cuo Zhang)*

B. Wang, C. Zhang and Z.Y. Dong are with the School of Electrical Engineering and Telecommunications, The University of New South Wales, Sydney, NSW 2052 Australia (e-mail: bo.w@student.unsw.edu.au, cuo.zhang@unsw.edu.au, zydong@ieee.org).

X. Li is with Jemena, Melbourne, VIC 3000 Australia (e-mail: esepco@126.com).

system operators (DSOs) aim to accommodate more rooftop PVs, excessive installations of rooftop PVs could exacerbate power unbalance and cause severe voltage rise during high PV power generation periods. Thus, the power unbalance and the voltage rise are major impediments that limit the network hosting capacity (HC) for PVs. HC is normally defined as the maximum DG capacity that can be connected to a network without causing any operating constraint violations **Error! Reference source not found.**.

To solve these issues, HC assessment can provide a sensible understanding about PV installations in DNs. In [1] and [3], sensitivity analysis-based methods are proposed to assess the maximum DG capacity by repetitively computing power flow with an increasing penetration level of renewable DG. Moreover, the authors in [4] and [5] apply optimal power flow (OPF)-based approaches to analyze the maximum network HC at candidate locations. However, these passive approaches have limited effects on HC improvement and cannot fully exploit the network potentials.

Recently, active network management (ANM) has been an effective means to exploit DG benefits, improve system reliability and postpone the network reinforcements. The main ANM schemes include voltage regulation, reactive power compensation, power factor control, DG curtailment and network reconfiguration [6]. Some research works study ancillary functions of DG itself in the planning stage. The authors in [6] evaluate the impacts of multi-DG configurations on the network HC. Besides, voltage/var control of PV inverters are considered in [7] and [8] to improve the network HC. On the other hand, some research works focus on the operation of controllable devices. The authors of [9] present an operation framework of DG curtailment, battery energy storage systems (BESSs) and flexible demand to minimize the operating cost and maximize the total energy export. Ref. [10] applies on-load tap changers (OLTCs), DG power factor control and DG curtailment to enhance HC with consideration of multiple scenarios. Furthermore, a robust coordinated strategy of OLTCs and static var compensators is proposed in [11] to maximize the HC. Static and dynamic network reconfiguration schemes are also studied in [12] to improve the HC.

However, there are several drawbacks in the existing works. Firstly, the works [1]-[12] assume a balanced DN when solving the HC improvement problems. But practical DNs are generally unbalanced. Secondly, the uncertain and random growth of future PV installations is not taken into account in **Error! Reference source not found.**-[12]. This uncertainty has considerable impacts on planning and operation of DNs, because the locations and capacities of the distributed rooftop PVs mainly depend on decisions of customers. In addition, most existing HC improvement methods aim to maximize the capacity of renewable DG subject to the network operating constraints. Using these methods for an unbalanced three-phase DN, DG will be equally allocated on the three phases to balance load power. From this point, these methods give ideal solutions of PV installations which may rarely occur in practice and the operating constraints cannot be guaranteed under other possible PV installation cases. Hence, the existing HC optimization methods are not suitable for the unbalanced DNs. Last but not least, the allocation of controllable distributed energy resources such as BESSs has not been optimized in [9]-[12], which may lead to low operating efficiency of the BESSs. The above issues leave research gaps and are expected to be addressed.

Considering the unbalanced DNs, it is necessary to integrate three-phase power flow model into the HC improvement problems. Ref. [13] introduces an iterative direct load flow approach to calculate three-phase power flow with two network topology matrices. However, due to the iteration process, it may result in a heavy computational burden. On the other hand, [14] proposes a branch flow model which can accurately model power flow. But it is not linear, leading to a high computational complexity and limited applications, such that it is expected to be linearized with some assumptions. Then, based on this branch flow model, an approximate linearized three-phase branch flow model is developed in [15]. This linearized model has a fast computational speed and high accuracy, and it has been applied to solve energy storage scheduling [16], microgrid restoration [17] and voltage/var control [18] problems. Thus, this paper adopts this linearized three-phase branch flow model for the HC improvement problem.

More importantly, to address the uncertainties, stochastic optimization (SO) [19] and robust optimization (RO) [20] methods have been widely used. The SO uses numerous sampled scenarios to model the uncertainties based on their probability distribution and optimizes the decision variables with these sampled scenarios. However, the probability distribution of the uncertainties is often unknown or inaccurate, and the computational burden of the SO is normally heavy. By contrast, the RO does not require the probability distributions of the uncertainties, but only needs their lower and upper bounds to construct uncertainty sets. Then, it searches the worst case within the uncertainty sets and obtains a robustly optimal solution under the worst case of uncertainty realization. The advantages of the RO include robust solutions against the uncertainties and high computing efficiency. Thus, the RO has attracted more attention and it is applied in this paper.

In addition, it is worth noting that the BESS operation is also considered in the BESS allocation problem, which forms a two-stage optimization problem [21]. Accordingly, an adaptive RO (ARO) method has been developed for such two-stage BESS allocation problem. The BESS operation model **Error! Reference source not found.** normally contains binary decision variables to indicate charging or discharging states, which are regarded as integer recourse variables. However, the widely used solution algorithms such as Bender decomposition [21] and column-and-constraint generation (CCG) [24] cannot directly solve the ARO problems with the integer recourse variables. Although some relaxation methods [25]-[28] have been developed to avoid the integer variables in the BESS models, their exactness is based on some assumptions and their application could be limited. For example, the relaxed models are designed for a single-phase BESS and their objectives are generally proportional to the BESS charging/discharging power. However, a three-phase BESS normally has the same

charging/discharging state for all three phases in practice. Thus, these relaxed methods are not suitable for the allocation problems of three-phase BESSs.

To solve the ARO problems with the integer recourse variables, a nested CCG algorithm [29] has been developed. As implied from its name, it solves the ARO problems by an outer-level and an inner-level CCG. Furthermore, the inner-level CCG relies on the enumeration of the integer recourse variables to search the worst case of uncertainty realization. As a result, the solving procedure could be inefficient and not suitable for a large-scale complex problem. Thus, a more efficient solution algorithm is required to solve the ARO problems with integer recourse variables. In [30], an alternating optimization procedure (AOP) algorithm is used to deal with a mixed integer linear programming (MILP) problem in a distributed algorithm framework. The AOP algorithm decomposes the original problem into an integer-decision-fixed problem and a continuous-decision-fixed problem, and then it solves these decomposed problems iteratively. A similar decomposition and alternation framework can be found in [31] to solve the bilinear term issue in the objective function. The advantage of these decomposition and alternation procedures is efficiently obtaining the optimal solution at a high convergence speed. Considering this feature, this paper aims to develop a new solution algorithm for the ARO problems with integer recourse variables by integrating the AOP algorithm.

In summary, the existing HC improvement works assume balanced distribution networks, neglect the uncertainties of future PV installations or do not consider the optimal allocation of BESSs. Moreover, the existing solution algorithms are inefficient for solving the ARO problems with the integer recourse variables. To address the above issues, this paper proposes a robust BESS allocation method to improve the HC of unbalanced DNs and develops a new solution algorithm.

Compared with the existing works, the main contributions of this paper are summarized as follows:

1) A BESS allocation method considering the uncertain PV power generation, loads and future PV installations is proposed to reduce power unbalance and alleviate voltage rise, and thus improve the HC of the unbalanced three-phase DNs.

2) With consideration of uncertain future PV installations and ARO application, a new insight into HC improvement is provided, which not only considers the worst power unbalance situation but also satisfies the allowed maximum PV capacity.

3) A new solution algorithm to solve the ARO problem with integer recourse variables is proposed and its high computing efficiency is verified.

II. Mathematical Formulation

This section introduces a BESS allocation optimization model which aims to minimize the power unbalance and mitigate the voltage rise, and thus improve the HC of the unbalanced three-phase DNs. Firstly, it is assumed that an initial evaluation of BESS investment has been conducted by the DSO. The investment cost is within a designed budget and the overall benefit is expected to be greater than the investment cost. Thus, the investment cost of BESSs is not considered in this paper. Secondly, each BESS unit is regarded as a single module with pre-designed parameters and the maximum number of BESS modules for installation is determinate. Also, multiple BESS modules can be installed at each candidate bus. As a result, this BESS allocation model determines the optimal numbers and locations of BESS modules at candidate buses. Detailed mathematical formulations are given in the following.

A. Battery Energy Storage Systems

BESSs can be used for power balance and voltage regulation to allow DNs to accommodate more distributed rooftop PVs. In this model, the BESS allocation and operating constraints are given as follows:

$$\alpha_i \in \{1, 2, 3\cdots K_i\}, \forall i \tag{1}$$

$$\sum_{i\in I} \alpha_i \le BSNo\,, \forall i \tag{2}$$

$$0 \le P^{ch}_{i,p,t} \le \alpha_i P^{ch}_{rate,i}, \forall i, p, t \tag{3}$$

$$0 \le P^{dis}_{i,p,t} \le \alpha_i P^{dis}_{rate,i}, \forall i, p, t \tag{4}$$

$$0 \le P^{ch}_{i,p,t} \le \beta_{i,t} K_i P^{ch}_{rate,i}, \forall i, p, t \tag{5}$$

$$0 \le P^{dis}_{i,p,t} \le (1-\beta_{i,t}) K_i P^{dis}_{rate,i}, \forall i, p, t \tag{6}$$

$$P^{BS}_{i,p,t} = P^{ch}_{i,p,t}\eta^{ch} - P^{dis}_{i,p,t}/\eta^{dis}, \forall i, p, t \tag{7}$$

$$E^{BS}_{i,t} = (1-\gamma)E^{BS}_{i,t-1} + \sum_{p\in P} P^{BS}_{i,p,t}\,\tau, \forall i, t \tag{8}$$

$$E^{BS}_{i,0} = E^{BS}_{i,24} \tag{9}$$

$$\alpha_i E^{cap}_i SoC_{min} \le E^{BS}_{i,t} \le \alpha_i E^{cap}_i SoC_{max}, \forall i, t \tag{10}$$

Constraint (1) states that the decisions of BESS allocations are integer variables and K_i BESS modules at maximum can be installed at each candidate bus. Constraint (2) indicates that the total number of BESS modules cannot exceed $BSNo$. Constraints (3) and (4) limit the BESS charging and discharging power within the allowed range by the integer variable α_i. Similarly, Constraints (5) and (6) restrict the BESS charging and discharging power within the allowed range by binary operation variables $\beta_{i,t}$ and only one state, i.e., charging or discharging, can be active for all three phases at each time interval. Moreover, Equation (7) computes the BESS internal power considering the charging and discharging efficiency. Equation (8) calculates the energy in the BESS during each time period considering energy leakage loss, and Equation (9) ensures that final stored energy in the BESS is equal to the initial one. Lastly, Constraint (10) guarantees the BESS SoC within the allowed operating range.

B. Linearized Three-phase Power Flow Model

Power flow is expected to be considered in the BESS allocation model as network operating constraints. The approximate linearized three-phase branch flow model [15] is applied in this paper and introduced as follows.

In this model, $\odot$ and $\oslash$ denote elementwise multiplication and division, respectively. Then, considering the three-phase branch flow from bus *i* to bus *k*, according to the Kirchhoff's voltage law, the voltage relationship between two buses can be modeled as:

$$\boldsymbol{V_k} = \boldsymbol{V_i} - \boldsymbol{z_{ik}}\boldsymbol{S^*_{ik}} \oslash \boldsymbol{V^*_i} \tag{11}$$

where $\boldsymbol{V_{i/k}} = \left[V^a_{i/k}, V^b_{i/k}, V^c_{i/k}\right]^T \in \mathbb{C}^{3\times 1}$ is bus voltage vector.

This article has been accepted for publication in a future issue of this journal, but has not been fully edited. Content may change prior to final publication. Citation information: DOI 10.1109/TPWRS.2020.3029532, IEEE Transactions on Power Systems

$\boldsymbol{S_{ik}} = \left[P_{ik}^a + jQ_{ik}^a, P_{ik}^b + jQ_{ik}^b, P_{ik}^c + jQ_{ik}^c\right]^T \in \mathbb{C}^{3\times 1}$ is branch power from bus *i* to bus *k*. And $\boldsymbol{z_{ik}} \in \mathbb{C}^{3\times 3}$ is branch impedance which consists of resistance $\boldsymbol{r_{ik}}$ and reactance $\boldsymbol{x_{ik}}$.

Multiplying both side of (11) by their complex conjugates, the following equation is obtained:

$$\boldsymbol{V_k} \odot \boldsymbol{V_k^*} = \boldsymbol{V_i} \odot \boldsymbol{V_i^*} - \boldsymbol{z_{ik}}\boldsymbol{S_{ik}^*} - \boldsymbol{z_{ik}^*}\boldsymbol{S_{ik}} + \boldsymbol{c}(\boldsymbol{V_i}, \boldsymbol{S_{ik}}, \boldsymbol{z_{ik}}) \tag{12}$$

where $\boldsymbol{c}(\boldsymbol{V_i}, \boldsymbol{S_{ik}}, \boldsymbol{z_{ik}})$ is the higher-order term. To implement linear approximation of the power flow, two assumptions are made by [15] and applied in this paper as

1) Line power loss is small, i.e., $\boldsymbol{c}(\boldsymbol{V_i}, \boldsymbol{S_{ik}}, \boldsymbol{z_{ik}}) \ll \boldsymbol{S_{ik}}$, and $\boldsymbol{c}(\boldsymbol{V_i}, \boldsymbol{S_{ik}}, \boldsymbol{z_{ik}})$ can be omitted.

2) Bus voltages are nearly balanced, then

$$V_i^a/V_i^b \approx V_i^b/V_i^c \approx V_i^c/V_i^a \approx e^{j2\pi/3} \tag{13}$$

Thus, by substituting (13) into (12) and ignoring $\boldsymbol{c}(\boldsymbol{V_i}, \boldsymbol{S_{ik}}, \boldsymbol{z_{ik}})$, (12) turns into

$$\boldsymbol{v_k} = \boldsymbol{v_i} - \bar{\boldsymbol{z}}_{\boldsymbol{ik}}\boldsymbol{S_{ik}^*} - \bar{\boldsymbol{z}}_{\boldsymbol{ik}}^*\boldsymbol{S_{ik}} \tag{14}$$

where $\boldsymbol{v_{i/k}} = [\,|V_{i/k}^a|^2, |V_{i/k}^b|^2, |V_{i/k}^c|^2]$, $\bar{\boldsymbol{z}}_{\boldsymbol{ik}} = \sigma \odot \boldsymbol{z_{ik}} \in \mathbb{C}^{3\times 3}$ and

$$\sigma = \begin{bmatrix} 1 & e^{-j2\pi/3} & e^{j2\pi/3} \\ e^{j2\pi/3} & 1 & e^{-j2\pi/3} \\ e^{-j2\pi/3} & e^{j2\pi/3} & 1 \end{bmatrix}.$$

With power balance constraints, the three-phase power flow for the proposed optimal BESS allocation model can be formulated as:

$$P_{n,p,t}^{br} = P_{n+1,p,t}^{br} + \tilde{P}_{n+1,p,t}^{LD} + P_{i,p,t}^{ch} - P_{i,p,t}^{dis} - \tilde{P}_{g,p,t}^{PV} - \delta_t \tilde{P}_{i,p}^{FPV}, \forall n, i, g, p, t \tag{15}$$

$$Q_{n,p,t}^{br} = Q_{n+1,p,t}^{br} + \tilde{Q}_{n+1,p,t}^{LD}, \forall n, p, t \tag{16}$$

$$\begin{bmatrix} v_{n+1,a,t} \\ v_{n+1,b,t} \\ v_{n+1,c,t} \end{bmatrix} = \begin{bmatrix} v_{n,a,t} \\ v_{n,b,t} \\ v_{n,c,t} \end{bmatrix} - \bar{\boldsymbol{z}}_{\boldsymbol{n\to n+1}} \begin{bmatrix} P_{n,a,t}^{br} - jQ_{n,a,t}^{br} \\ P_{n,b,t}^{br} - jQ_{n,b,t}^{br} \\ P_{n,c,t}^{br} - jQ_{n,c,t}^{br} \end{bmatrix} - \bar{\boldsymbol{z}}_{\boldsymbol{n\to n+1}}^* \begin{bmatrix} P_{n,a,t}^{br} + jQ_{n,a,t}^{br} \\ P_{n,b,t}^{br} + jQ_{n,b,t}^{br} \\ P_{n,c,t}^{br} + jQ_{n,c,t}^{br} \end{bmatrix}, \forall n, t \tag{17}$$

where δ_t in (15) denotes the PV profile of future PV installations, which is assumed to be the mean values of all existing PV profiles, and $(\tilde{\cdot})$ represents uncertainty. Equations (15) and (16) calculate the branch active and reactive power flow, respectively. Finally, Equation (17) computes the square of bus voltage magnitude.

C. BESS Allocation Optimization Model

Combined with the above BESS and power flow models, the proposed BESS allocation optimization model is given as follows:

$$min \sum_{t\in T} P_t^{unb} \tag{18}$$

s.t. (1)-(10), (15)-(17)

$$|P_{1,a,t}^{br} - P_{1,b,t}^{br}| \le P_t^{unb}, \forall t \tag{19}$$

$$|P_{1,b,t}^{br} - P_{1,c,t}^{br}| \le P_t^{unb}, \forall t \tag{20}$$

$$|P_{1,c,t}^{br} - P_{1,a,t}^{br}| \le P_t^{unb}, \forall t \tag{21}$$

$$V_{min}^2 \le v_{n,p,t} \le V_{max}^2, \forall n, p, t \tag{22}$$

$$P_{1,p,t}^{br\ 2} + Q_{1,p,t}^{br\ 2} \le P_{max}^{TF\ 2}, \forall t \tag{23}$$

$$P_t^{unb} \le UNB_{max} \tag{24}$$

Considering power unbalance and voltage rise caused by excessive PV installations, the objective function (18) is to minimize the total active power unbalance at the root branch (transformer low-voltage side), while bus voltages are constrained within the allowed range. Actually, the distribution network is regarded as a three-phase load to the up-stream grid. The heavily unbalanced load will cause high neutral current and significantly increase power loss during power transmission. Moreover, for distribution transformer, the unbalanced load will cause zero sequence current which leads to local temperature rise, transformer aging acceleration and operational risk. Thus, as the grid code requires, the three-phase power flow at root branch is expected to be as balanced as possible. With this objective, more distributed rooftop PVs can be accommodated in the DNs without violating the operating constraints, such that the HC of the unbalanced DNs can be improved.

In addition, Constraints (19)-(21) indicate the root branch unbalance at each time interval. Constraint (22) limits the bus voltage within the allowed range. Then, Constraint (23) ensures that the apparent power at root branch cannot exceed the transformer power limit. The feasible region formed by the real power and reactive power is a circle, so that (23) can be linearized by a polygonal inner approximation method [32]. Lastly, Constraint (24) restricts the hourly root branch unbalance within UNB_{max}.

Overall, in this optimization model, the objective function (18) subject to Constraints (1)-(10), (15)-(17) and (19)-(24) forms a MILP problem. The decision variables are the BESS allocations α_i and the uncertainties are $\tilde{P}_{n,p,t}^{LD}$, $\tilde{P}_{g,p,t}^{PV}$ and $\tilde{P}_{i,p,t}^{FPV}$.

III. Adaptive Robust Optimization For BESS Allocation

In DNs, the locations and the capacities of the distributed rooftop PVs depend on customers' decisions. Therefore, besides loads and existing PV power generation, the capacity of future PV installations should also be considered as the uncertainty in the BESS allocation problem. To achieve robust decisions against the uncertainties, this paper develops an ARO model for the proposed BESS allocation method. There are two optimization stages, i.e. a planning optimization stage and an operation optimization stage. The former determines the optimal allocation of BESS while the latter handles the optimal BESS dispatch under the worst case of the uncertainty realization. Therefore, the solution can give a new insight into future PV installations that likely lead to the worst case of power unbalance. This means that DSOs may avoid such PV installations. Moreover, according to the principle of RO, if the feasible solutions with the identified worst case can be obtained, other possible future PV installations including allowed maximum PV capacity from the uncertainty set will be satisfied as well. In other words, the solution of the proposed method for HC improvement can also achieve the maximum capacity for the future PV installations.

A. Uncertainty Set

Uncertain loads, existing PV power generation and future

PV installations are modelled as uncertainty sets which contain lower and upper bounds of the uncertainties as well as adjustable uncertainty budgets, given as follows.

$$U_{LD/PV/HC} = \{P_{n,p,t}^{LD/PV/FPV}: \quad (25)$$

$$\underline{P}_{n,p,t}^{LD/PV/FPV} \le P_{n,p,t}^{LD/PV/FPV} \le \overline{P}_{n,p,t}^{LD/PV/FPV} \quad (25a)$$

$$\underline{\mu}_p^{LD/PV/FPV} \le \frac{\sum_{n\in N}\sum_{t\in T} P_{n,t}^{LD/PV/FPV}}{\sum_{n\in N}\sum_{t\in T} \hat{P}_{n,t}^{LD/PV/FPV}} \le \overline{\mu}_p^{LD/PV/FPV}\} \quad (25b)$$

Constraint (25a) denotes that the uncertainty variables can vary within the lower and upper bounds. Then, Constraint (25b) states the overall uncertainty degree at each phase must be limited within the uncertainty budgets, and it can be calculated by the ratio of the summation of uncertainty variables to the summation of expected uncertainty values. It is noteworthy that the budget interval will enlarge if $\underline{\mu}_p$ decreases and $\overline{\mu}_p$ increases. As a result, the solution will be more robust against the uncertainties, but also more conservative for the objective.

In addition, lower and upper bounds of loads and existing PV power generation can be determined via historical data or interval prediction techniques [33]. Moreover, to evaluate the impact of future PV installations on HC, the lower and upper bounds of future PV installations can be set as an expected minimum capacity and an allowed maximum capacity respectively, considering the grid code. For example, if the allowed maximum PV capacity for a household customer is 5kW and there are 3 non-PV customers connecting to a bus at phase A, the corresponding lower and upper bounds of the future PV installations can be set as 0 and 15kW, respectively. Moreover, the budget interval can be set based on the DSO's preferred PV penetration level.

B. Adaptive Robust Optimization Model

To solve the proposed BESS allocation model with uncertainties, it is formulated into the following ARO compact matrix model:

$$\min_{x}\ \max_{u}\ \min_{y,z}\ a^T y \quad (26)$$

$$\text{s.t.} \quad Bx \le c \quad (26a)$$

$$Dx + Ey + Fz \le g \quad (26b)$$

$$Hx + Iy + Ju = k \quad (26c)$$

$$u \in U \quad (26d)$$

In this ARO model, $\boldsymbol{x}$ represents the planning decision variables which are integer variables of BESS allocation. Then $\boldsymbol{y}$ denotes the continuous operation variables that include BESS output power decisions and other dependent variables such as power flow and unbalance variables. Furthermore, $\boldsymbol{z}$ stands for the integer operation variables which are BESS operation states. Note that $\boldsymbol{z}$ is also called integer recourse variables. Lastly, $\boldsymbol{u}$ represents the uncertainty variables.

In objective (26), the first "*min*" is to minimize the unbalance by optimizing the BESS allocation, which represents planning optimization. Similarly, the second "*min*" is to minimize the unbalance by optimizing the BESS operation. Then the "*max*" is to seek the worst case of the uncertainty realization in the given uncertainty sets. Thus, the combination of "*max-min*" represents operation optimization which is to minimize the unbalance under the worst case by adjusting BESS operation variables. In addition, Constraints (1) and (2) can be converted to (26a). Constraints (3)-(6), (10) and (19)-(24) can be grouped in (26b). Constraints (7)-(9) and (15)-(17) form (26c), and Constraint (26d) requires the uncertainty variables to satisfy uncertainty sets (25).

IV. Solution Algorithm

The ARO problem has a form of tri-level "*min-max-min*" which indicates these three optimization levels interact with each other. It normally requires a decomposition and alternation process to solve. It is indicated by [24] that the CCG algorithm has fast convergence speed and high efficiency. However, the conventional CCG algorithm requires the ARO model with continuous recourse variables only. But the proposed ARO model also includes integer recourse variables.

To efficiently solve the ARO with integer recourse variables, this paper proposes a CCG with the AOP (CCG-AOP) algorithm. This algorithm contains two solving loops. The outer loop has the similar structure and procedure to the conventional CCG. While the inner loop applies the AOP algorithm [30] to efficiently seek the worst case with the feasible solution of the integer recourse variables.

Firstly, the outer loop of the proposed CCG-AOP decomposes the proposed ARO model into an outer-level master problem and an outer-level subproblem with the integer recourse variables.

The ***outer-level master problem, M^o*** is given as

$$\min_{x,y,z}\ \eta \quad (27)$$

$$\text{s.t.} \quad Bx \le c \quad (27a)$$

$$\eta \ge a^T y_l, \forall 1 \le l \le L \quad (27b)$$

$$Dx + Ey_l + Fz_l \le g, \forall 1 \le l \le L \quad (27c)$$

$$Hx + Iy_l + Ju_l^* = k\ , \forall 1 \le l \le L \quad (27d)$$

where l denotes the l-th iteration and L denotes the current iteration number of the outer-level CCG-AOP. In this outer-level master problem, with the fixed uncertainty variables u_l^* from the outer-level subproblem, the optimal solutions including a group of x^* and L groups of (y_l^*, z_l^*) are obtained. Then outer-level lower bound (LB^o) is updated and x^* is passed to the outer-level subproblem.

The ***outer-level subproblem, S^o*** is expressed as

$$\max_{u}\ \min_{y,z}\ a^T y \quad (28)$$

$$\text{s.t.} \quad Dx^* + Ey_l + Fz_l \le g \quad (28a)$$

$$Hx^* + Iy_l + Ju_l = k \quad (28b)$$

$$u_l \in U \quad (28c)$$

The outer-level subproblem is solved with the fixed decisions x^* from the outer-level master problem. As a result, the outer-level upper bound (UB^o) is updated and the result of u_{l+1}^*, regarded as a newly identified worst case, is achieved. Afterwards, with this identified worst case u_{l+1}^* and newly created variables (y_{l+1}, z_{l+1}), a group of constraints in the form of (27b) to (27d), as CCG cuts, are added to the outer-level master problem for the next iteration.

It notes that directly solving the outer-level subproblem is challenging, especially when the integer decision variables are involved. Thus, the inner loop of the proposed CCG-AOP algorithm decomposes the outer-level subproblem into an in-

teger-fixed problem and an uncertainty-fixed problem and solve these two decomposed problems iteratively.

By taking the strong duality to the inner "*min*" problem in (28), the ***integer-fixed problem*** is obtained as

$$\max_{u} \pi^T(Dx^* + Fz^* - g) + \rho^T(Hx^* + Ju - k) \quad (29)$$

$$\text{s.t.} \quad a + E^T\pi + I^T\rho = 0 \quad (29a)$$

$$u \in U, \pi \geq 0, \quad (29b)$$

where π and ρ are dual variables, x^* and z^* are the optimal results of the outer-level master problem and the uncertainty-fixed problem respectively. Note that the integer-fixed problem is bilinear and it can be solved by an outer approximation (OA) method [21]. In consequence, the worst case of the uncertainties is obtained as u^* and it is passed to the uncertainty-fixed problem. Moreover, the inner-level upper bound (UB^I) is updated.

The ***uncertainty-fixed problem*** can be written as

$$\min_{y,z} a^T y \quad (30)$$

$$\text{s.t.} \quad Dx^* + Ey + Fz \leq g \quad (30a)$$

$$Hx^* + Iy + Ju^* = k \quad (30b)$$

where x^* and u^* are the optimal solutions of the outer-level master problem and integer-fixed problem respectively. Model (30) is solved to obtain the optimal solutions of y^* and z^* but only z^* is passed to the integer-fixed problem. The inner-level lower bound (LB^I) is also updated

Thus, the integer-fixed problem and the uncertainty-fixed problem are solved iteratively until the gap between LB^I and UB^I is less than the inner-level terminal threshold ϵ^I. The result u^* is regarded as the newly identified worst case, i.e. u_l in (28), and it will be delivered to the outer-level master problem.

The outer-level master problem and the outer-level subproblem are also solved iteratively until the gap between the LB^o and UB^o is less than the outer-level terminal threshold ϵ^o.

The detailed solving procedures of the outer and inner loops are described in Algorithm I and II and Fig. 1.

It is worth noting that solving the tri-level "*min-max-min*" ARO model is in NP-hard [24], and naturally, no global optimum can be guaranteed. However, by applying the proposed CCG-AOP algorithm, the ARO problem with the integer recourse variables can be efficiently solved and a local optimum can be obtained.

ALGORITHM I
CCG-AOP OUTER LOOP ALGORITHM

Initialization: set l=1, u_l=u_0, ϵ^o=ϵ_0, UB^o=+∞ and LB^o=-∞.
While l < Maximum iteration number
1. Solve outer-level master problem, obtain x_l^* and z_l^* update UB^o.
2. Check convergence when $l \geqslant 2$:
if $(UB^o - LB^o)/UB^o \leqslant \epsilon^o$ **or** $x_l^* = x_{l-1}^*$, **Then** *break*.
3. Solve outer-level subproblem with x_l^*, obtain u_{l+1}^* and update LB^o. Then add constraints with newly created variables (y_{l+1}, z_{l+1}) and u_{l+1}^* in the form of (27b)-(27d) to the outer-level master problem for next iteration.
End While
Return x_l^*

ALGORITHM II
CCG-AOP INNER LOOP ALGORITHM

Initialization: set r=1, x=x_l^*, z=z_l^*, ϵ^I=ϵ_0, UB^I=+∞ and LB^I=-∞.
While r < Maximum iteration number
1. Solve the integer-fixed problem with z^*, obtain u_r^* and update UB^I.
2. Solve the uncertainty-fixed problem with u_r^*, obtain z_{r+1}^* and update LB^I.
3. Check convergence: **if** $(UB^I - LB^I)/UB^I \leqslant \epsilon^I$, **Then** *break*.
End While
Return u_r^*.

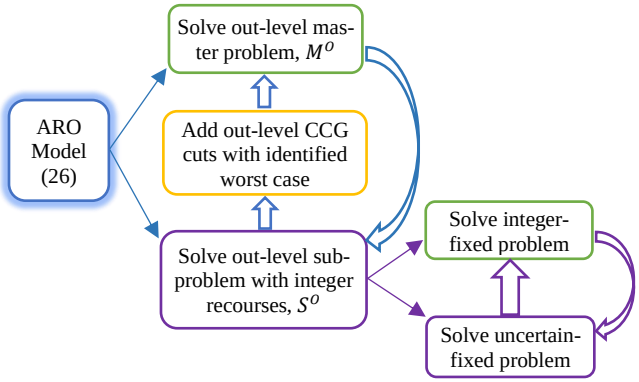

Fig. 1 Proposed CCG-AOP algorithm.

V. CASE STUDY

To comprehensively verify effectiveness and efficiency of the proposed BESS allocation method and the CCG-AOP solution algorithm, two IEEE standard distribution testing systems are utilized for numerical simulations. Various tests focusing on different BESS numbers, allocation methods, operation feasibility and solution algorithms are implemented.

All the numerical simulations are conducted on a 3.4GHz CPU and 16GB RAM desktop. The proposed optimization model is programmed on Matlab 2017b platform with Yalmip toolbox R20190425 [34] and solved by Gurobi 8.1 [35].

A. IEEE 34-Bus Test System

Firstly, the proposed BESS allocation method is tested on an IEEE 34-bus three-phase distribution system [36]. The network topology is shown in Fig. 2. In addition, the allowed bus voltage range is set as [0.95 1.05] p.u. The maximum unbalance limit UNB_{max} is set as 0.18 p.u. Furthermore, the capacity of each BESS module is set as 120kW/240kWh with 95% charging and discharging efficiency. Maximum 6 BESS modules can be installed at six candidate buses (808, 832, 840, 844, 848, 860), circled in Fig. 2, and at most 3 BESS modules can be installed at each candidate bus. The BESS SoC range is set as [0.1 0.9]. The daily initial SoC of BESSs is set as 50%.

In this test system, the profiles of aggregated loads and existing PV power generation are given in Fig. 3. The lower and upper bounds are set as 0.8 and 1.2 of the expected PV power generation and loads. Moreover, the maximum PV capacity that can be installed at each bus is set as 1.5 of the bus loads. In terms of the uncertainty budgets, the lower and upper budgets are set as 0.9 and 1.1 for the PV power generation and

This article has been accepted for publication in a future issue of this journal, but has not been fully edited. Content may change prior to final publication. Citation information: DOI 10.1109/TPWRS.2020.3029532, IEEE Transactions on Power Systems

loads, 0.2 and 1.8 for future PV installations.

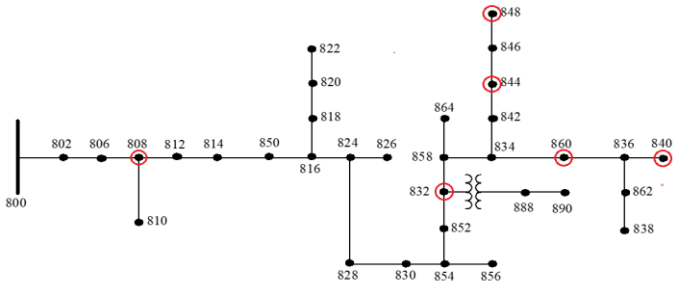

Fig. 2 IEEE 34-bus distribution network topology.

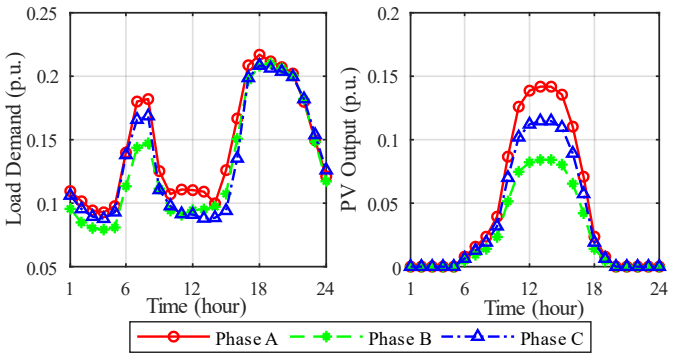

Fig. 3 Aggregated load and existing PV profiles.

1) BESS Allocation and Hosting Capacity

With Model (26) solved, the optimal BESS allocations are obtained and shown in Fig. 4. By installing BESS modules at buses 840, 848 and 860, the total power unbalance under the worst case is minimized as 1.07 p.u.

Moreover, the results of the future PV installations under the worst case are illustrated in Fig. 5 and summarized in Table I. For the future rooftop PVs, installing most of them at Phases C could cause the worst power unbalance situation, so that DSO should avoid installing such many distributed PVs at Phases C. Note that the allowed maximum future PV installations defined by the uncertainty set can also be achieved with these BESS allocation results.

Accordingly, the root branch power flow and power unbalance over the day are depicted in Fig. 6. It shows that the critical unbalance occurs during the period of high PV power generation. It is worth noting that the power unbalance under the worst case is kept within the limits.

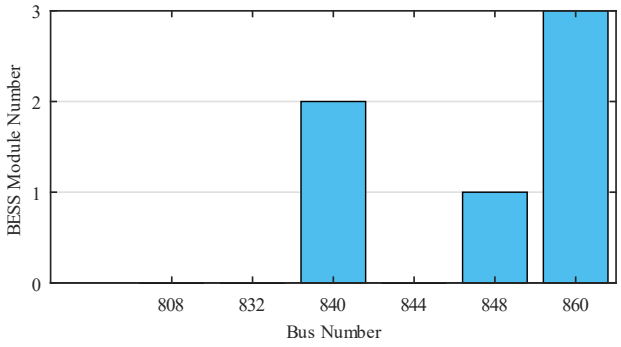

Fig. 4 BESS allocations of the proposed method.

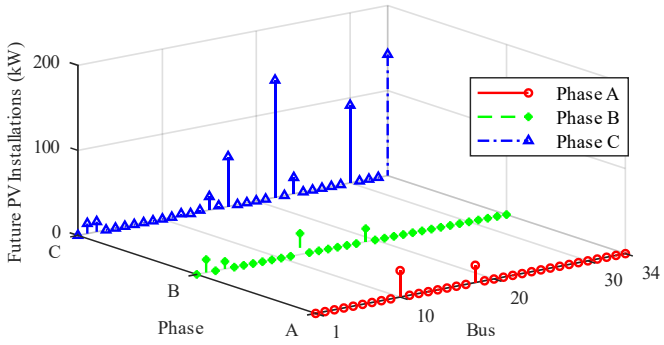

Fig. 5 Future PV installation under the worst case.

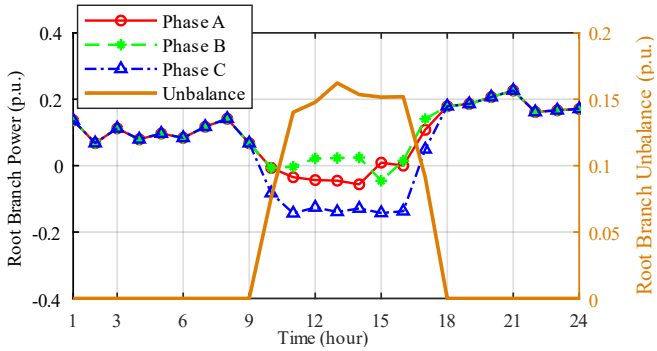

Fig. 6 Root branch power flow and unbalance.

TABLE I
PV INSTALLATION RESULTS OF THE PROPOSED METHOD

Phase	Existing PV Installations (kW)	Future PV Installations (kW)	Total PV Installations (kW)	Total PV Penetration Rate
A	393.9	51.5	445.4	73.5%
B	233.6	64.2	297.8	51%
C	318.5	495.0	813.5	140.5%

2) BESS Operation under Worst Case

Under the worst case of uncertainty realization, the BESS SoC and charging/discharging power are also optimized and shown in Fig. 7 and Fig. 8, respectively. From these two figures, it can be found that from midnight to morning, BESSs charge or discharge to maintain the power balance. As the PV power generation increases in the morning, the BESSs charge at Phases C to limit the voltage rise and reduce the power unbalance, because most PVs are installed at Phases C. Afterwards, the BESSs charge or discharge to fulfill the loads and reduce the power unbalance. Eventually, the BESS SoC returns to the initial SoC for the daily operation requirement.

This article has been accepted for publication in a future issue of this journal, but has not been fully edited. Content may change prior to final publication. Citation information: DOI 10.1109/TPWRS.2020.3029532, IEEE Transactions on Power Systems

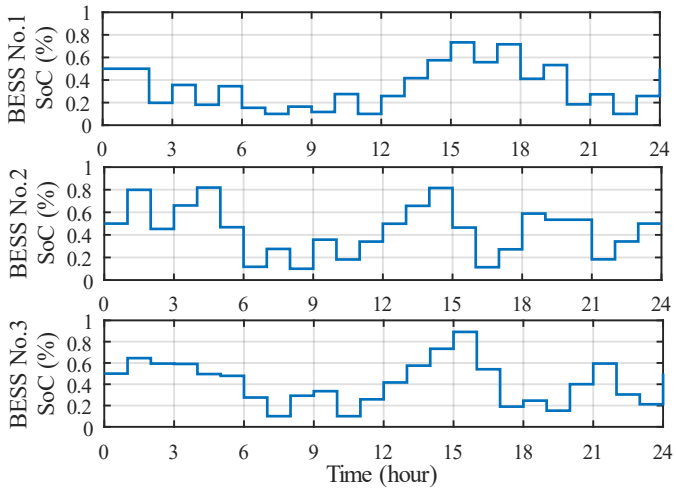

Fig. 7 BESS SoC under the worst case.

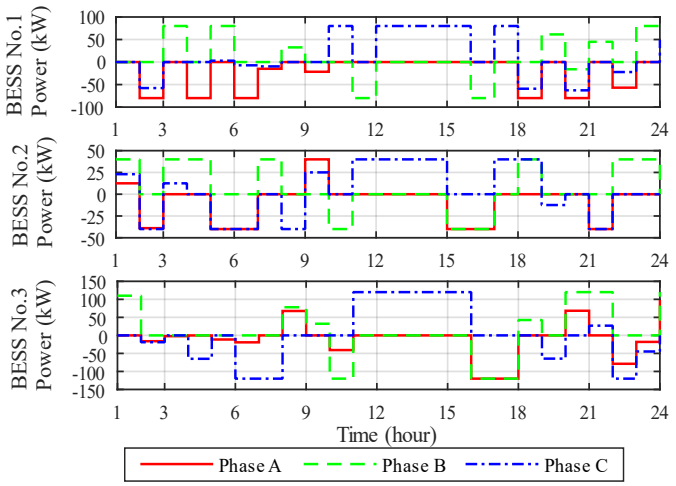

Fig. 8 BESS output power under the worst case.

3) Power Unbalance with Different BESS Numbers

To evaluate the impact of the maximum number of BESS modules, different values of $BSNo$ are used and tested. The results are summarized in Table II.

TABLE II
COMPARISON OF DIFFERENT VALUES OF $BSNo$

$BSNo$ Value	Total Power Unbalance (p.u.)	BESS Allocation					
		808	832	840	844	848	860
5	No solution	-	-	-	-	-	-
6	1.07	0	0	2	0	1	3
7	0.95	0	2	1	1	1	2
8	0.82	0	1	1	2	1	3

In Table II, there is no solution when setting $BSNo$ to be 5, indicating that constraint satisfaction under the worst case cannot be met with 5 BESS modules or less. In addition, as $BSNo$ increases, the total power unbalance is reduced by optimally allocating the BESS modules at different buses. Thus, considering the minimum number of BESSs to achieve solutions, 6 BESS modules are suggested.

4) Comparison with Other Methods

To highlight the advantages of the proposed BESS allocation method over the existing methods, the following two methods are applied and tested for comparison.

Method A: Maximizing the HC for the future PV installations, subject to the BESS and network operating constraints without considering uncertainties, given as below.

$$max \sum_{i\in I}\sum_{p\in P} P_{i,p}^{FPV} \tag{31}$$

s.t. (1)-(10), (15)-(17) and (19)-(24)

Note that the expected loads and existing PV power generation are used in Method A, which forms a deterministic optimization problem.

Method B: Similar to Method A, but the uncertainties of the loads and existing PV power generation are considered and modelled as the uncertainty sets with the same settings in Section V.A. The problem is solved by the proposed CCG-AOP algorithm.

Through the optimization, the BESS allocation results of Methods A and B are shown in Fig. 9. Method A allocates one BESS module at bus 840 and 848, respectively. Since Method B takes the uncertainties into account, two BESS modules are installed at bus 848 and 860, respectively to improve operation robustness.

With these BESS installations, the comparison of PV installation results is summarized in Table III. It can be found that both Methods A and B achieve the allowed maximum capacity for the future PV installations.

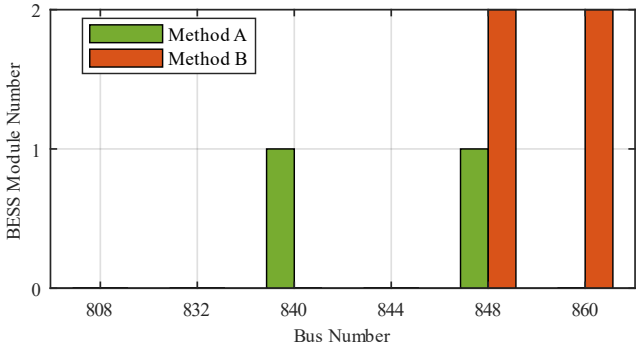

Fig. 9 BESS allocations of Methods A and B

TABLE III
COMPARISON OF PV INSTALLATION RESULTS WITH DIFFERENT METHODS

Phase	Existing PV Installations (kW)	Future PV Installations (kW)		
		Method A	Method B	Proposed Method
A	393.9	463.6	463.6	51.5
B	233.6	578.1	578.1	64.2
C	318.5	495.0	495.0	495.0

Compared to the proposed BESS allocation method, the locations and numbers of the installed BESS modules are different, due to the different objective functions and optimization methods. The existing methods aim to maximize the HC by optimally allocating the BESS modules. As a result, although this optimized HC can be achieved, other possible future PV installations cannot be guaranteed. This is because Methods A

This article has been accepted for publication in a future issue of this journal, but has not been fully edited. Content may change prior to final publication. Citation information: DOI 10.1109/TPWRS.2020.3029532, IEEE Transactions on Power Systems

and B only provide feasible solutions for the maximum HC. On the other hand, the proposed method minimizes the root branch power unbalance considering the future PV installations as uncertainties. Since the worst case of the future PV installations is considered, the BESS allocation results should also be valid for other possible PV installations.

Besides, when the BESS allocation results of the proposed method are substituted back to the worst case of Method B, the allowed maximum PV capacity can also be achieved as that in Method B. It illustrates that even though the proposed method does not directly provide the maximum HC, its results can also satisfy the allowed maximum PV capacity. By contrast, when the BESS allocation results of Methods A and B are applied to the worst case found in the proposed method, there is no feasible solution. This is mainly because the uncertainties of future PV installations are not considered, which shows an advantage of the proposed method over the existing methods.

5) Feasibility Check

To verify the effectiveness and robustness of the proposed method, 2000 scenarios are randomly generated within the lower and upper bounds by Monte Carlo sampling. The uniform probability distribution is applied for the uncertainties of loads, existing PV power generation and future PV installations. Each scenario represents one uncertainty realization case. In this stage, by fixing the BESS allocations, the BESS daily operation is optimized. The BESS allocation results of the proposed method with different values of $BSNo$, as well as those of Methods A and B are tested for comparison. The average power unbalance and solution infeasibility rate are calculated for each method. Note that for the infeasible scenarios, they are recomputed without the unbalance and voltage limits. The results are given in Table IV.

TABLE IV
FEASIBILITY CHECK RESULTS AND COMPARISONS

		Average Power Unbalance (p.u.)	Infeasibility Rate (%)
Method A		0.260	13.5%
Method B		0.134	8.35%
Proposed Method	with 6 BESS modules	0.089	0
	with 7 BESS modules	0.073	0
	with 8 BESS modules	0.058	0

In Table IV, the average power unbalance of the proposed method is the lowest, followed by Methods B and A. Moreover, the infeasibility rate of Method A is highest due to no consideration of the uncertainties. By contrast, the infeasibility rate of Method B is reduced significantly, but still exists. This is because the uncertainties of future PV installations are not considered. However, the proposed method can fully eliminate infeasibility under the uncertainties. Moreover, as $BSNo$ increases in the proposed method, the average power unbalance reduces.

In summary, the proposed BESS allocation approach can effectively enhance the operational robustness under the uncertainties and reduce the power unbalance.

6) Computing Efficiency

This section compares the computing efficiency of the proposed CCG-AOP and the conventional nested-CCG algorithms [29] for solving the ARO Model (26). Since the main difference between these two algorithms is how to solve the "*max-min*" subproblem with integer recourses, the details of the iteration number, the solving time and the optimal objective result for the subproblem are given in Table V.

As shown in Table V, the solving time of the subproblem is significantly reduced with the fewer iterations by the proposed CCG-AOP algorithm, due to the avoidance of the enumeration of the integer recourses. Thus, the proposed CCG-AOP algorithm can achieve high computing efficiency.

TABLE V
COMPARISON OF SOLUTION ALGORITHMS FOR SUBPROBLEM

Solution Algorithm	**CCG-AOP**	**Nested-CCG**
Iteration No.	[1, 2]	[1; 1, 2]
Solving Time (s)	[0.72, 0.76]	[0.77, 0.56, 2.12]
Total Time (s)	1.48.	3.33
Optimal Objective (p.u.)	1.07	1.07

B. IEEE 123-Bus Test System

To indicate the scalability of the proposed BESS allocation method and solution algorithm, a larger and more unbalanced IEEE 123-bus three-phase distribution system [36] is used to conduct simulations. Its topology as well as the profiles of aggregated loads and existing PV power generation are shown in Fig. 10 and Fig. 11, respectively. The parameters of BESS module are set as 150kW/300kWh with 95% charging and discharging efficiency. Also, maximum 6 BESS modules can be installed at five candidate buses (29, 51, 60, 76, 97), circled in Fig. 10 and each candidate bus can accommodate 3 BESS modules at most. Moreover, the unbalance limit UNB_{max} is set as 0.2 p.u. The uncertainty budgets for future PV installations are set as 0.3 and 1.8. Other settings are the same as those in Section V.A.

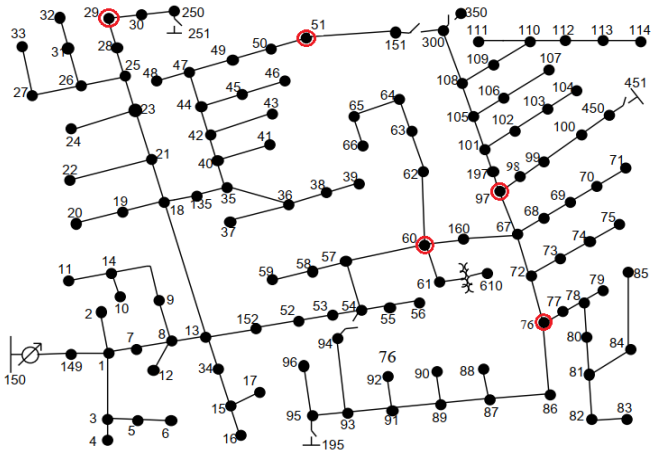

Fig. 10 IEEE 123-bus distribution network topology.

This article has been accepted for publication in a future issue of this journal, but has not been fully edited. Content may change prior to final publication. Citation information: DOI 10.1109/TPWRS.2020.3029532, IEEE Transactions on Power Systems

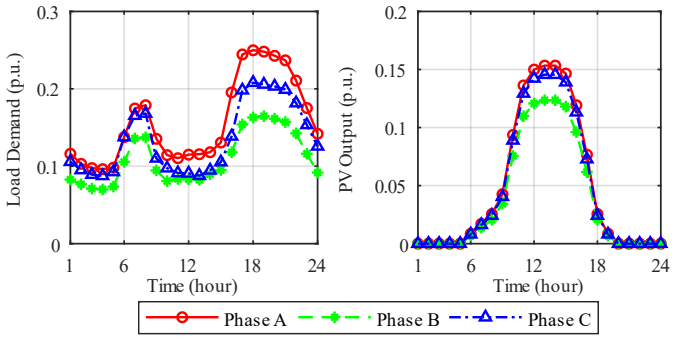

Fig. 11 Aggregated load and existing PV profiles.

1) BESS Allocation and Hosting Capacity

By optimization, the BESS allocation results are illustrated in Fig. 12, showing that BESS modules are installed at buses 29, 51, 60 and 76. Meanwhile, the total power unbalance under the worst case is 1.79 p.u.

In addition, the worst case of future PV installations is given in Fig. 13, which describes that installing most of distributed rooftop PVs at Phases B and C could cause the worst power unbalance.

Then, the root branch power flow and power unbalance results are depicted in Fig. 14. It indicates that the significant power unbalance occurs in the afternoon and the unbalance cannot be eliminated in the evening under the worst case, due to the lower loads at Phase B.

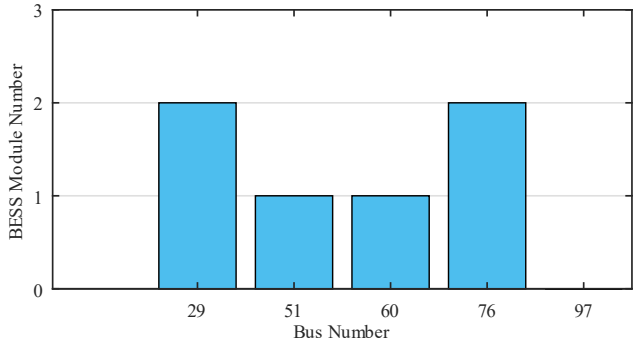

Fig. 12 BESS allocations of the proposed method.

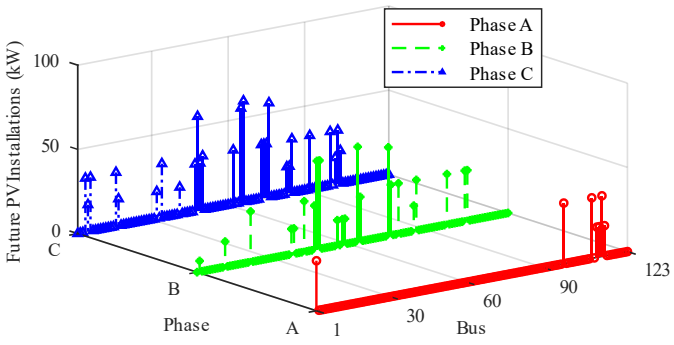

Fig. 13 Future PV installation under the worst case.

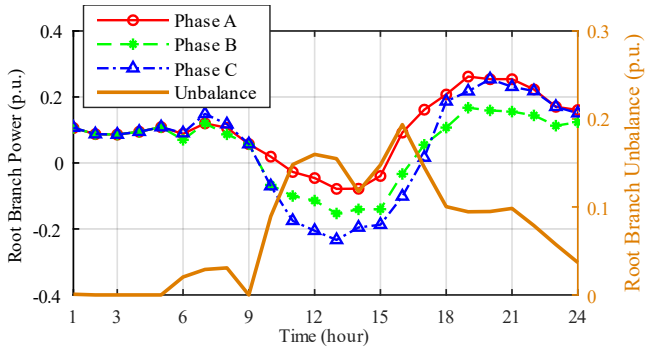

Fig. 14 Root branch power flow and unbalance.

2) Power Unbalance with Different BESS Numbers

Furthermore, different values of the maximum BESS number, $BSNo$, are used and tested for comparison.

The results are given in Table VI. It shows that there is no solution when setting $BSNo$ to be 5, which indicates that with 5 BESS modules or less, the operating constraints cannot be guaranteed. Besides, as $BSNo$ increases, the total power unbalance can be further reduced by allocating more BESS modules. Thus, to meet the network operation requirement with the minimum number of BESS modules, 6 BESS modules are suggested.

TABLE VI
COMPARISON OF DIFFERENT VALUES OF $BSNo$

$BSNo$ Value	Total Power Unbalance (p.u.)	BESS Allocation				
		29	51	60	76	97
5	No solution	-	-	-	-	-
6	1.79	2	1	1	2	0
7	1.59	2	1	1	1	2
8	1.53	2	0	3	2	1

3) Feasibility check

For this system, similar to Section V.A, the feasibility check is conducted with random 2000 scenarios of the uncertainty realization. The BESS allocation results with different values of $BSNo$ are tested for comparison, given in Table VII.

It shows that all the BESS allocation solutions achieve zero infeasibility rate for all the scenarios. Besides, the average power unbalance decreases as $BSNo$ increases. Thus, the results verify that the proposed BESS allocation method has high operational robustness against uncertainty realization and high efficiency to reduce the power unbalance.

TABLE VII
FEASIBILITY CHECK RESULTS AND COMPARISONS

		Average Power Unbalance (p.u.)	Infeasibility Rate (%)
Proposed Method	with 6 BESS modules	0.149	0
	with 7 BESS modules	0.091	0
	with 8 BESS modules	0.056	0

4) Computing Efficiency

To further illustrate the high computing efficiency of the proposed CCG-AOP in a larger system, it is compared with the nested-CCG algorithms [29] in terms of computing time for solving the subproblem. The detailed information of the

iteration number, the solving time and the optimal objective value is summarized in Table VIII.

In Table VIII, the solving time of the subproblem is significantly reduced with the fewer iterations by the proposed CCG-AOP algorithm. In summary, the proposed CCG-AOP algorithm is applicable to a larger system and it can effectively improve the computing efficiency.

TABLE VIII
COMPARISON OF SOLUTION ALGORITHMS FOR SUBPROBLEM

Solution algorithm	CCG-AOP	Nested-CCG
Iteration No.	[2]	[3]
Solving Time(s)	[4.41]	[15.224]
Total Time(s)	4.41	15.224
Optimal Objective (p.u.)	1.79	1.79

VI. CONCLUSION

This paper proposes a robustly optimal BESS allocation method, aiming to reduce the power unbalance and alleviate the voltage rise, and in turn improve the HC of the unbalanced three-phase DNs. In this method, besides loads and existing PV power generation, future PV installations are considered as the uncertainties. As a result, a new insight into HC improvement is provided, which not only considers the worst power unbalance but also satisfies the allowed maximum PV capacity. In addition, to solve the proposed ARO problem with integer recourse variables, this paper develops a CCG-AOP algorithm. The simulation results verify the high efficiency and robustness of the proposed method.

In future works, a full planning procedure of BESSs, including sizing, locating and investment minimization will be considered in the proposed robust HC improvement model.

VII. REFERENCES

[1] B. Wang, C. Zhang, K. Meng, et. al., "Improving hosting capacity of unbalanced distribution networks via battery energy storage systems," *in Proc. 11th IEEE PES Asia-Pacific Power and Energy Engineering Conference (APPEEC 2019)*, Macao, Dec. 2019, pp. 1-5.

[2] F. Ding, B. Mather, "On distributed PV hosting capacity estimation sensitivity study and improvement," *IEEE Trans. Sustain. Energy*, vol. 8, no. 3, pp. 1010-1020, Jul. 2017.

[3] R.A. Kordkheili, B. Bak-Jensen, J. R. Pillai, P. Mahat, "Determining Maximum Photovoltaic Penetration in a Distribution Grid considering Grid Operation Limits," *PES General Meeting Conference & Exposition*, 2014.

[4] G. P. Harrison, A. R. Wallace, "Optimal power flow evaluation of distribution network capacity for the connection of distributed generation," *IET Proc. Generat. Transm. Distrib.*, vol. 152, no. 1, pp. 115-122, Jan. 2005.

[5] C. J. Dent, L. F. Ochoa, G. P. Harrison, "Network distributed generation capacity analysis using OPF with voltage step constraints," *IEEE Trans. Power Syst.*, vol. 25, no. 1, pp. 296-304, 2010.

[6] S. S. Al Kaabi, H. H. Zeineldin, V. Khadkikar, "Planning active distribution networks considering multi-DG configurations," *IEEE Trans. Power Syst.*, vol. 29, no. 2, pp. 785-793, Mar. 2014.

[7] S. S. AlKaabi, V. Khadkikar, H. H. Zeineldin, "Incorporating PV inverter control schemes for planning active distribution network," *IEEE Trans. Sustain. Energy*, vol. 6, no. 4, pp. 1224-1233, Oct. 2015.

[8] N. C. Tang, G. W. Chang, "A stochastic approach for determining PV hosting capacity of a distribution feeder considering voltage quality constraints," *18th Int.Conf. Harmonics and Quality of Power*, 2018.

[9] S. Gill, I. Kockar, G. Ault, "Dynamic optimal power flow for active distribution networks," *IEEE Trans. Power Syst.*, vol. 29, pp. 1-11, 2014.

[10] L.F. Ochoa, C.J. Dent, G.P. Harrison, "Distribution Network Capacity Assessment: Variable DG and Active Networks," *IEEE Trans. Power Syst.*, vol. 25, pp. 87-95, 2010.

[11] S. Wang, S. Chen, L. Ge, L. Wu, "Distributed generation hosting capacity evaluation for distribution systems considering the robust optimal operation of OLTC and SVC," *IEEE Trans. Sustain. Energy*, vol. 7, no. 3, pp. 1111-1123, Jul. 2016.

[12] F. Capitanescu, L. F. Ochoa, H. Margossian and N. D. Hatziargyriou, "Assessing the potential of network reconfiguration to improve distributed generation hosting capacity in active distribution systems," *IEEE Trans. Power Syst.*, vol. 30, no. 1, pp. 346–356, Jan. 2015.

[13] Jen-Hao Teng, "A direct approach for distribution system load flow solutions," *IEEE Trans. Power Delivery*, vol. 18, no. 3, pp. 882-887, July 2003.

[14] M. Farivar, S. H. Low, "Branch flow model: Relaxations and convexification," *IEEE Trans. Power Syst.*, vol. 28, no. 3, pp. 2554-2564, Aug. 2013

[15] L. Gan and S. H. Low, "Convex relaxations and linear approximation for optimal power flow in multiphase radial networks," in Proc. 2014 Power Syst. Comput. Conf., Wroclaw, Poland, 2014, pp. 1–9.

[16] Z. Wang, A. Negash and D. S. Kirschen, "Optimal scheduling of energy storage under forecast uncertainties," *IET Generation, Transmission & Distribution*, vol. 11, no. 17, pp. 4220-4226, Dec. 2017.

[17] B. Chen, C. Chen, J. Wang, K. L. Butler-Purry, "Sequential service restoration for unbalanced distribution systems and microgrids," *IEEE Trans. Power Syst.*, vol. 33, no. 2, pp. 1507-1520, Mar. 2018.

[18] R. R. Jha, A. Dubey, C. Liu and K. P. Schneider, "Bi-Level Volt-VAR Optimization to Coordinate Smart Inverters With Voltage Control Devices," *IEEE Trans. Power Syst.*, vol. 34, no. 3, pp. 1801-1813, May 2019.

[19] L. Wu, M. Shahidehpour and T. Li, "Stochastic Security-Constrained Unit Commitment," *IEEE Trans. Power. Syst.*, vol. 22, no. 2, pp. 800-811, May 2007.

[20] C. Zhang, Y. Xu and Z. Y. Dong, "Probability-Weighted Robust Optimization for Distributed Generation Planning in Microgrids," *IEEE Trans. Power. Syst.*, vol. 33, no. 6, pp. 7042-7051, Nov. 2018.

[21] H. Yang et al., "Optimal Wind-Solar Capacity Allocation With Coordination of Dynamic Regulation of Hydropower and Energy Intensive Controllable Load," *IEEE Access*, vol. 8, pp. 110129-110139, 2020.

[22] B. Wang, C. Zhang and Z. Y. Dong, "Interval Optimization Based Coordination of Demand Response and Battery Energy Storage System Considering SoC Management in A Microgrid," *IEEE Trans. Sustain. Energy*, vol. 11, no. 4, pp. 2922-2931, Oct. 2020.

[23] D. Bertsimas, E. Litvinov, X. A. Sun, J. Zhao, and T. Zheng, "Adaptive robust optimization for the security constrained unit commitment problem," *IEEE Trans. Power Syst.*, vol. 28, pp. 52-63, 2013.

[24] B. Zeng and L. Zhao, "Solving two-stage robust optimization problems using a column-and-constraint generation method," *Operations Research Letters*, vol. 41, no. 5, pp.457-461, Sept. 2013.

[25] S. K. K. Hari, K. Sundar, H. Nagarajan, R. Bent and S. Backhaus, "Hierarchical Predictive Control Algorithms for Optimal Design and Operation of Microgrids," *2018 Power Systems Computation Conference (PSCC)*, Dublin, 2018, pp. 1-7.

[26] K. Garifi, K. Baker, D. Christensen and B. Touri, "Convex Relaxation of Grid-Connected Energy Storage System Models with Complementarity Constraints in DC OPF," *IEEE Transactions on Smart Grid*, April 2020.

[27] Z. Li, Q. Guo, H. Sun and J. Wang, "Storage-like devices in load leveling: Complementarity constraints and a new and exact relaxation method", *Appl. Energy*, vol. 151, pp. 13-22, Aug. 2015.

[28] H. Yang and H. Nagarajan, "Optimal Power Flow in Distribution Networks under N−1 Disruptions: A Multi-stage Stochastic Programming Approach," CNLS at Los Alamos National Laboratory, NM, United States, 2020.

[29] L. Zhao and B. Zeng, "An exact algorithm for two-stage robust optimization with mixed integer recourse problems," University of South Florida, Working Paper, 2011.

[30] Z. Li, M. Shahidehpour and W. Wu, et al., "Decentralized Multiarea Robust Generation Unit and Tie-Line Scheduling Under Wind Power Uncertainty," *IEEE Trans. Sustain. Energy*, vol. 6, no. 4, pp.1377-1388, Oct. 2015.

[31] Á. Lorca and X. A. Sun, "The Adaptive Robust Multi-Period Alternating Current Optimal Power Flow Problem," *IEEE Trans. Power Syst.*, vol. 33, no. 2, pp. 1993-2003, March 2018.

[32] C. Zhang, Y. Xu and Z. Y. Dong, "Robustly Coordinated Operation of a Multi-Energy Micro-Grid in Grid-Connected and Islanded Modes Under

Uncertainties," *IEEE Trans. Sustain. Energy*, vol. 11, no. 2, pp. 640-651, April 2020.
[33] C. Wan, Z. Xu, P. Pinson, Z. Y. Dong, and K. P. Wong, "Probabilistic forecasting of wind power generation using extreme learning machine," *IEEE Trans. Power Syst.*, vol. 29, no. 3, pp. 1033–1044, 2014.
[34] J. Löfberg, "YALMIP: A toolbox for modeling and optimization in MATLAB," *Proc. IEEE Int. Symp. Comput. Aided Control Syst. Design*, New Orleans, LA, USA, pp. 284–289, 2004.
[35] GUROBI. [Online]. Available: http://www.gurobi.com.
[36] "IEEE Distribution Test Feeders," [Online]. Available: https://site.ieee.org/pes-testfeeders/resources/.

Bo Wang (S'19) received the B.E. (Honours) and M.S. degrees from the University of New South Wales in 2013 and in 2014 respectively. He is currently pursuing the Ph.D. degree in electrical engineering at the University of New South Wales. His research interests include microgrid planning and operation, voltage stability and control, and applications of machine learning.

Cuo Zhang (S'16-M'19) received the B.E. (Hons.) degree in electrical (power) engineering from the University of Sydney, Australia in 2014 and the Ph.D. degree in electrical engineering from the University of New South Wales, Australia in 2018. He is now the research associate with the University of New South Wales, Australia. He is also a chief investigator of ARC Research Hub for Integrated Energy Storage Solutions. His research interests include power system planning and operation, voltage stability and control, microgrids, multi-energy systems, and applications of optimization theory and artificial intelligence in these areas. He was a recipient of 2 IEEE PES General Meeting Best Conference Papers, IEEE Transactions on Smart Grid Best Reviewer for 2019, UNSW Promoting High Quality Research Papers Scheme Award, and the 2014 University Medal from the University of Sydney.

Zhao Yang Dong (M'99–SM'06-F'17) received Ph.D. degree from the University of Sydney, Australia in 1999. He is currently a SHARP professor and Director of UNSW Digital Grid Futures Institute at the University of New South Wales, Australia. He was previously Ausgrid Chair and Director of the Ausgrid Centre for Intelligent Electricity Networks, the University of Newcastle, Australia and Head of School of Electrical and Information Engineering, the University of Sydney, Australia. He also worked as manager for system planning with Transend Networks (now TASNetworks), Australia. His research interests include smart grid, power system planning and stability, renewable energy systems, electricity market, and computational methods for power engineering applications. He has served/is serving as an editor for a number of IEEE Transactions and IET journals. He is a Fellow of the IEEE and a Web of Science Highly Cited Researcher.

Xuejun Li received Master degree of electric power system from Shandong University, China, Ph.D degree from Beijing Jiaotong University, China and MBA degree from the University of Sydney, Australia. Dr. Li is currently Deputy Executive General Manager of Jemena and looks after gas and electricity T&D network assets. His research interests include asset management, information system management, and project management. He is Charted Engineer and member of IET (The Institute of Engineer and Technology).